Structural Analysis of a Potassium Hollandite $K_{1.35}Ti_8O_{16}$

T. VOGT

Institut Laue Langevin, B.P. 156X, 38042 Grenoble Cedex, France

E. SCHWEDA*, C. WÜSTEFELD, AND J. STRÄHLE

Institut für Anorganische Chemie, Universität Tübingen, Auf der Morgenstelle 18, D-74 Tübingen, Federal Republic of Germany

AND A. K. CHEETHAM

Chemical Crystallography Laboratory, University of Oxford, 9 Parks Road, Oxford OX 3PD, United Kingdom

Crystals of $K_{1.35}Ti_8O_{16}$ have been investigated by single-crystal X-ray analysis, X-ray powder patterns, electron diffraction, and high-resolution electron microscopy. $K_{1.35}Ti_8O_{16}$ is obtained in the form of dark blue tetragonal crystals of the space group $I4/m$ having the hollandite structure with $a = 1018.8(2)$ pm and $c = 296.61(7)$ pm. The refinement converges to a reliability factor of 0.025. The occupation of the $T(2,2)$ tunnel sites in potassium is not statistical. Incommensurate one-dimensional superstructures were found by powder diffraction patterns as well as by electron diffraction. The multiplicity calculated from powder X-ray diffraction is $m = 5.79$ and that found by electron diffraction is $m = 8.1$; this is explained in terms of beam damage and loss of potassium within the $T(2,2)$ sites. The final step in the decomposition is the formation of rutile from $K_{1.35}Ti_8O_{16}$ when all the potassium atoms are lost in the tunnels. © 1989 Academic Press, Inc.

Introduction

Hollandite minerals have been studied in recent years as nuclear waste immobilizers and as model systems for fast ionic conductors. The general hollandite formula is $A_x(B_yTi_{8-y})O_{16}$ with $A = K$, Cs, and Ba. B is either a divalent or a trivalent cation such as Mg^{2+}, Mn^{2+}, Al^{3+}, or Ti^{3+}, occupying sites within the oxygen octahedra. The hollandite structure first reported by Bystroem

and Bystroem [1] can be described as columns of four linear strings of edge-sharing octahedra parallel to the c-axis (see Fig. 1). The structure can be deduced from the rutile structure by an alternately clockwise and anticlockwise cooperative rotation by 45° of the above-mentioned four linear strings of corner-sharing octahedra [2]. The chains of octahedra are linked together, forming a framework of continuous parallel tunnels aligned along the c-axis. These tunnels are either 2×2 or 1×1 octahedra in cross section. A maximum of two A cations

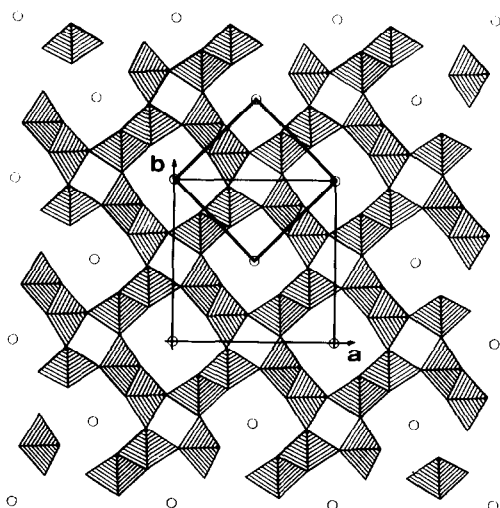---

* To whom correspondence should be addressed.

FIG. 1. STRUPLO plot along [001] with the unit cell and the structural features marked in the high-resolution image. Circles are the potassium atoms in the 2 × 2 tunnels of the titanium oxygen framework.

per unit cell may be located in the larger tunnels. In many hollandites, crystal chemical considerations require only partial occupancy of these tunnel sites and the vacant and occupied sites are usually ordered. In the simplest case, systematic occupancy sequences along individual tunnels are correlated with those in neighboring tunnels and constitute one-dimensional superstructures. More commonly, however, the vacant and occupied tunnel sites along several neighboring tunnels are similarly ordered and correlated, forming regular three-dimensional arrays. These superstructures give rise to characteristic diffuse intensities and superlattice reflections in electron diffraction patterns (edp). The average dimensions of the superstructure measured along the tunnels, its multiplicity, can also be deduced from edp. A supercell is said to be commensurate when its dimensions correspond to integral multiples of those of the basic unit cell (or subcell). Many hollandites, however, exhibit incommensurate, i.e., nonintegral, superstructures. The hol-

landite system $K_x(Ti_x^{III}Ti_{8-x}^{IV})O_{16}$ has been discussed by Beyeler and Schuler (3). They prepared $K_{1.54}(Ti_{1.54}^{III}Ti_{6.46}^{IV})O_{16}$ by direct synthesis. However, no crystallographic parameters have been determined until now.

Single-Crystal Structure Determination

Experimental

The synthesis of hollandite single-crystals was accomplished by slow O_2 oxidation of a potassium–titanium–nitride–fluoride precursor, which was obtained by ammonolysis of K_2TiF_6 at 600°C. The reaction was carried out in a quartz tube in streaming argon at 1200°C. At the given temperature there is notable oxygen diffusion through the quartz tube, so that nitrogen and fluorine will be completely replaced by oxygen. Slow O_2 oxidation was for the benefit of single crystals. Light element analysis by analytical electron microscopy (4) confirmed that no nitrogen and fluorine remained in the product.

From a single crystal mounted on quartz glass fiber, Buerger precession photographs were taken to establish the symmetry. This revealed a tetragonal unit cell with Laue symmetry $4/m$ and systematic absences for reflections h, k, l with $h + k + l = 2n + 1$. This reduces the possible spacegroups to $I4/m, I\bar{4}$, or $I4$.

A suitable crystal ($0.1 \times 0.1 \times 0.3$ mm) was mounted onto an automatic Syntex four-circle diffractometer with the c-axis approximately aligned with the ϕ-axis of the diffractometer. Unit cell dimensions and a crystal orientation matrix were obtained by least-squares refinement of 20 centered reflections between $35 \geq 2\theta \geq 65$. The intensities were collected in an ω-scan mode using MoKα radiation and a graphite monochromator. The reflections $(14\bar{1})$, $(\bar{1}41)$, and $(\bar{4}1\bar{1})$ were used as standards and measured every 100 reflections. During the measurement they showed a maximum and

minimum intensity ratio of 1.0207 and 0.9993, respectively, which implies no significant intensity variation. Between $3 \geq 2\theta \geq 78$ 1995 reflections (excluding 78 standards) were measured over two octants in reciprocal space; two of these were rejected, one on the basis of an asymmetric profile, the other because it was a spike.

The data were corrected for Lorentz and polarization effects. After sorting and merging, 549 reflections were used to refine 23 parameters. The internal reliability factor $R_{int} = \Sigma[|F^2 - F^2_{mean}|]/\Sigma F^2$ was 0.0096. A Patterson map and subsequent tangent expansion refinements using SHELX-76 revealed that the structure was of the hollandite type. In the full matrix least-squares refinement unit weights were used and no absorption or extinction corrections were applied. Using anisotropic temperature factors for all atoms the refinement converged to a reliability factor of 0.025 based on structure factors and 0.033 based on squared structure factors. The results of the refinement are shown in Table II. The analysis of the $F_{obs} - F_{calc}$ values showed that for 15 reflections the deviation was bigger than 2σ. All refinements were carried out on a VAX 8650 using the SHELX 76 program (5).

Discussion

The general formula for hollandite-type structures $A_x(B_y Ti_{8-y})O_{16}$ with $0.7 \leq x \leq 1.2$ and $0.1 \leq y \leq 0.5$ (1) shows that the framework has a net negative charge due to partial substitution of di- or trivalent ions for Ti^{4+} which is compensated by the type A cations. In our case this leads to the stoichiometry $K_{1.35}Ti^{3+}_{1.35}Ti^{4+}_{6.65}O_{16}$. Applying the method of Brown and Altermatt (6) to obtain the bond valence parameters, the valence of Ti was found to be 3.89 using $r_0 = 1.815$ and $B = 0.37$. This agrees quite well with the average charge calculated from the stoichiometry based on the refined site oc-
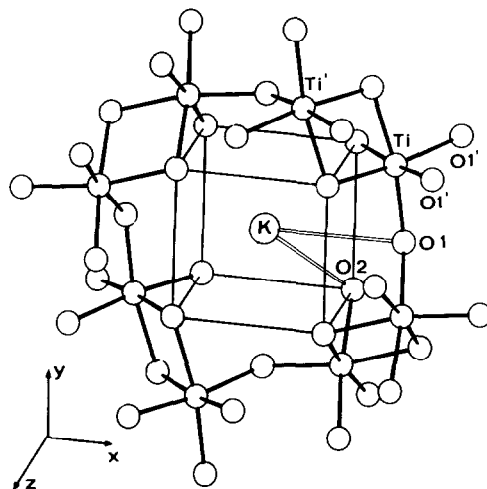

FIG. 2. ORTEP plot showing the octahedral matrix of the hollandite-type structure. The tunnel site is occupied by a potassium atom, which is coordinated by eight O(2) and four O(1).

cupation factor, which gives rise to an average charge of 3.83 per titanium.

Examination of the octahedra reveals that they are distorted. The shared octahedral edges are significantly shorter. The titanium atoms are displaced from the centers of the octahedra and moved along its threefold axis leading to three short and three longer Ti–O bonds. The distances are similar to those observed in other hollandite type structures and are listed in Table I (see Fig. 2). By comparison of the frame-

TABLE I

INTERATOMIC DISTANCES IN $K_{1.35}Ti_8O_{16}$ GIVEN IN pm

	K–K'	296.61		Ti–O(1)	193.2(2)
8×	K–O(2)	301.22	2×	Ti–O(1)'	197.6(1)
4×	K–O(1)	342.5(2)	2×	Ti–O(2)	198.1(1)
4×	K–Ti	372.33	2×	Ti–O(2)'	200.9(2)
				Ti–Ti'	303.68(1)
			2×	Ti–Ti'	296.61
	O(1)–O(2)'	261.1(3)		O(2)–O(2)'	258.9(2)
2×	O(1)–O(2)	281.5(2)		O(2)–O(2)'	296.6
2×	O(1)–O(2)	287.9(3)			
4×	O(1)–O(1)'	287.3(3)		Ti–O$_{average}$	197.5
2×	O(1)–O(1)'	296.1			

work structure of the Ti^{3+}/Ti^{4+} hollandite with an Al^{3+}/Ti^{4+} potassium hollandite (7), a significant decrease in the average Ti–O bond length from 197.6 to 195.3 pm is observed which also causes a decrease in the eight K–O distances from 301.2 to 297.8 pm. This might be due to the longer Ti^{3+}–O bond compared to the Al^{3+}–O bond. In our case the Ti–O bond length is very similar to that of a $Mg^{2+}Ti^{4+}$ framework determined by Cheary (8).

The cations in the holes of the hollandite framework are coordinated by eight equivalent oxygen atoms at the corners of a tetragonal prism and it is known from the literature (9) that they are disordered over equivalent positions resulting in a wide compositional range of this class of compounds. The cations are displaced from the $2b$ sites in the tunnel axis due to repulsive forces between themselves. Beyeler (10) has analyzed the diffuse X-ray scattering visible in reciprocal lattice planes perpendicular to the c^*-axis, showing that the diffuse scattering is basically independent of the framework and is due only to the disordered cations which form a supercell of four sites, the empty site having the adjacent cation moved toward the vacancy. On setting the sof (site occupation factor) of the $2b$ position at 0.125, implying full occupancy, the refinement converged only to R values of 0.0365 and 0.0565 based on structure factors and squared structure factors, respectively. Upon refinement of the sof, an occupancy of 66.6% ± 1.0% was found with a significant improvement in the reliability factors (0.0249, 0.0328). This led to a correlation of 61% between the sof and the U33 thermal parameter, still small enough to regard the results as significant. The deviation from full occupancy is well known and it was Abriel (11) who pointed out the correlation between sof and U33. The less occupied the $2b$ position is, the higher the value of U33, the component of the thermal parameter parallel to the c-axis indicating

structural disorder. In our case U33 was 0.29 $Å^2$, which means that the root-mean-square amplitude was about 0.5 Å along the c-axis. This agreed well with those observed by Abriel for $K_{1.8}V_8O_{16}$ (0.26 $Å^2$) having 89.6 ± 1.6% occupancy and for $Tl_{1.75}V_8O_{16}$ (0.252 $Å^2$) having 87.2 ± 0.6% occupancy. Calculations with a split atom model displacing some of the K atoms from the $2b$ position at (0 0 $\frac{1}{2}$) to a $4e$ position at (0 0 $\pm z$), keeping only the fourfold axis, converged to reliability factors of 0.0226 and 0.0316 for structure factors and squared structure factors, respectively. The z parameters of the off-site potassiums were allowed to vary together with the site occupation factors and the anisotropic Debye–Waller factors. This led to enormous correlations and should be judged critically. The positional and thermal parameters of the framework were not affected. Table II shows the results for the two potassium atoms. The z position of the off-centered potassium $z = 0.68(3)$ agrees quite well with $z = 0.700(2)$ for $K_{1.50}Al_{1.50}Ti_{6.5}O_{16}$ (7) and with other off-centered positions quoted in the literature. It is also in agreement with the observation of Beyeler and Schuler (3)

TABLE II

FINAL POSITIONAL PARAMETERS AND COEFFICIENTS OF THE ANISOTROPIC TEMPERATURE FACTORS OF $K_{1.35}Ti_8O_{16}$

| | Positional parameters for split atom model | | | |
	x	y	z	sof
Ti	0.1501	0.6668	0.50000	0.50000
O1	−0.0396(2)	0.6662(2)	0.50000	0.50000
O2	−0.2956(2)	0.6564(2)	0.50000	0.50000
K1	0.00000	0.00000	0.50000	0.03(1)
K2	0.00000	0.00000	0.68(3)	0.05(1)

| | Coefficients of the anisotropic temperature factors for split atom model | | | | | |
	U11	U22	U33	U23	U13	U12
Ti	0.0065(1)	0.0073(1)	0.0070(1)	0.0000	0.0000	−0.0013(1)
O1	0.0051(5)	0.0106(6)	0.0082(6)	0.0000	0.0000	−0.0003(5)
O2	0.0065(5)	0.0056(5)	0.0079(6)	0.0000	0.0000	0.0005(4)
K1	0.026(5)	0.026(5)	0.04(2)	0.0000	0.0000	0.0000
K2	0.016(2)	0.016(2)	0.11(3)	0.0000	0.0000	0.0000

that the displacement is inversely proportional to the size of the monovalent cation, where a $\Delta z = 0.24$ is quoted for K^+. The cation is displaced along c to minimize the repulsive electrostatic forces by moving toward neighboring vacancies. Refining only off-site positions led to the following parameters for potassium: $x = 0.0$, $y = 0.0$, $z = 0.574(3)$ with site occupation factor $0.0845(1)$. This final refinement converged to $R = 0.0249$ and $R = 0.0328$.

Powder Diffraction

Experimental

A Guinier film of crushed crystals was indexed with a tetragonal cell with $a = 1018.8(2)$ pm and $c = 296.61(7)$ pm. These values were obtained by least-squares refinements of the cell constants and a linear overall zero-point shift. The cell dimensions were later used in the least-squares refinement of the single-crystal data.

Discussion

The positions of the Bragg reflections were determined by using Si as an internal standard. The film was scanned with a standard microdensitometer. Table III shows the results of the indexing and gives the $2\theta_{obs}2\theta_{calc}$ list. However there are two peaks in the Guinier film which could not be indexed by the simple tetragonal cell. One has a 2θ value of $21.417°$, corresponding to a d value of 414.0 pm; the other has values of $43.328°$ and 208.5 pm. If one indexes the first peak on the basis of the tetragonal cell under the assumption that it is a reflection of the $(1\ 0\ l)$ type, a miller index of $(1\ 0\ 0.65)$ is obtained. For the second peak, under the assumption that it is a $(2\ 0\ l)$ type, one obtains $(1\ 0\ 1.29)$. This corresponds to the observation of Beyeler (10), who observed a diffuse sheet that was situated 0.22 reciprocal lattice units (rlu) from the Bragg spots perpendicular to the c^*-axis

TABLE III

GUINIER DIFFRACTION PATTERN OF $K_{1.35}Ti_8O_{16}$

h k l	$2\theta_{obs}$	$2\theta_{calc}$	Difference
1 1 0	12.253	12.258	−0.005
2 0 0	17.363	13.376	−0.012
2 2 0	24.675	24.677	−0.001
3 1 0	27.660	27.646	0.014
4 0 0	36.183	35.187	−0.004
1 2 1	36.103	36.084	0.019
3 3 0	37.396	37.399	−0.003
4 2 0	39.523	39.505	0.018
3 0 1	40.343	40.320	0.024
3 2 1	44.223	44.214	0.009
5 1 0	45.330	45.331	−0.001
1 4 1	47.842	47.854	−0.012
6 0 0	53.922	53.933	−0.011
4 3 1	54.544	54.578	−0.034
5 2 1	57.703	57.732	−0.029
0 0 2	62.552	62.562	−0.010
4 5 1	66.631	66.626	0.005
1 3 2	69.740	69.727	0.012
3 7 0	70.312	70.289	0.023

for $K_{1.54}Mg_{0.77}Ti_{7.23}O_{16}$, which is 1 rlu $= 1/c^*$. This implies that the ordering is predominantly one-dimensional in $K_{1.54}Mg_{0.77}Ti_{7.23}O_{16}$. The irrational l index is related to the multiplicity m to describe superlattices in hollandites. For the $(1\ 0\ l)$ type, this is simply given by the relation $m = 2/(1 - l)$. For the first reflection this leads to $m = 5.7916$, which is in good accordance with values that Bursill and Grzinic (12) have found for barium hollandites. They observed that for $x \geq 1.2$ the multiplicity increases continuously from 5 toward 6 and that the superlattice is commensurate only for $x = 1.2$ and $m = 5.00$. Cheary (8), analyzing barium magnesium hollandites, found that the observed multiplicity of 5.85 rather than 6.00 at $x = 1.33$ implies the formation of domains whose boundaries affect the 2θ position of the superlattice lines. From the X-ray analysis we conclude that there is an incommensurate one-dimensional ordering of the cations along the [001] direction with a multiplicity of 5.79
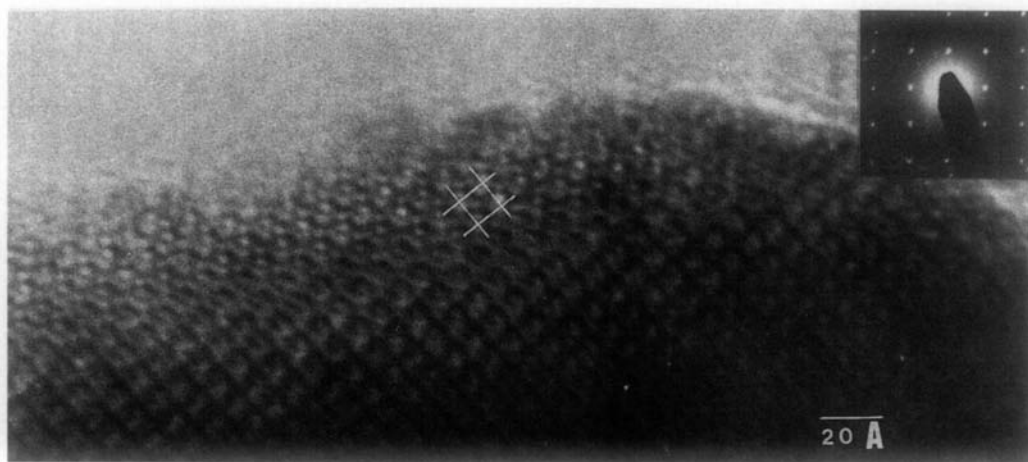
FIG. 3. High-resolution electron microscope image of $K_{1.35}Ti_8O_{16}$ along the [001] direction. In the upper-right corner is the electron diffraction pattern.

and an occupancy of 66% and the supercell has a c-axis three times that of the tetragonal one. The cations are arranged in sequences of vacancy $\cdots (K^+ \cdots K^+) \cdots$ vacancy, thus creating layers of entirely empty tunnels in the ab-plane.

High-Resolution Electron Microscopy and Electron Diffraction

Experimental

Single crystals of $K_{1.35}Ti_8O_{16}$ were crushed and supported on a holey carbon copper grid. Electron micrographs were taken on a Philips EM 420 high-resolution microscope equipped with a field emission gun and operated at 100 keV (13) using a double tilt $\pm25°$ goniometer from Gatan. Analytical electron microscopy was performed on a JEOL 2000 FX equipped with a Tracor Northern ultrathin window X-ray detector.

Discussion

Structural investigations of hollandites using electron microscopy have been extensively described by Kesson and White (14, 15) and Bursill and Grzinic (12). Figure 3 shows the thin crystal which was oriented along (001) in order to obtain structural resolution. The image was recorded at optimum defocus (Scherzer defocus). In the thin part of the crystal the contrast may be interpreted directly in terms of the local projected structure. In the STRUPLO plot (Fig. 1) (16) thin lines show the unit cell and thick lines display the same structural feature as those marked in the HREM image. The black contrast corresponds to the Ti atoms in the centers of two edge-sharing oxygen octahedra. The image displays the hollandite structure.

Both the selected area diffraction patterns and the high-resolution images were found to change within the electron beam during observation. Figure 4 shows a diffraction pattern for the ($\bar{1}11$) zone of $K_{1.35}$ Ti_8O_{16}. The calculated multiplicity is $m = 8.1$. However, it is possible that the intense electron beam of the field emission gun, although a small condensor aperture was used, has altered the superlattice periodicity during the exposure of the crystal. Typically this would mean an increase in multiplicity and this is an explanation for
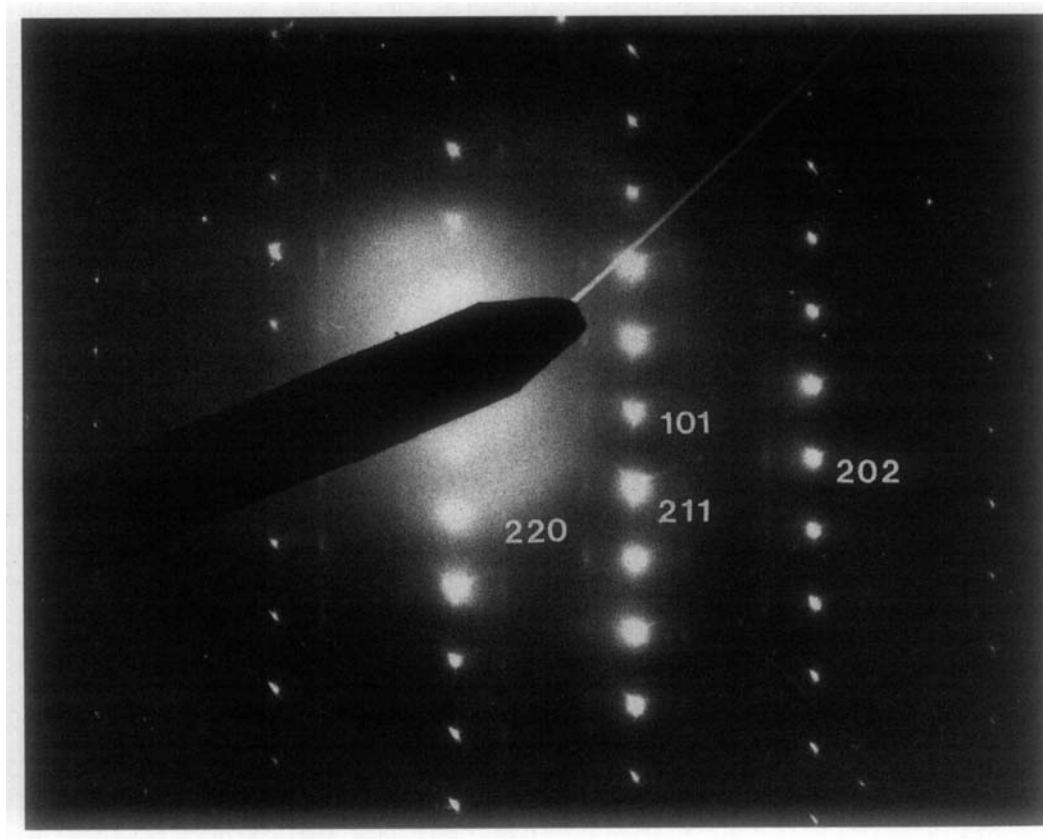
FIG. 4. Electron diffraction pattern of the ($\bar{1}11$) zone displaying the incommensurate superstructure with multiplicity $m = 8.1$.

the different results for the multiplicity calculated from powder X-ray diffraction and from the observed [$\bar{1}11$] zone in the electron diffraction pattern. Of about 40 investigated crystals, superstructures have been observed being in most cases incommensurate and one-dimensional. Intensive beam heating for 10 min using no condenser aperture caused the collapse of the structure and the formation of rutile. This is caused by the complete loss of cations in the tunnels.

Acknowledgments

References

1. A. BYSTROEM AND A. M. BYSTROEM, *Acta Crystallogr.* 3, 146 (1950).
2. L. A. BURSILL, *Acta Crystallogr. B* 35, 530–538 (1979).
3. H. U. BEYELER AND SCHULER, *Solid State Ionics* 1, 77 (1980).
4. A. K. CHEETHAM, A. J. SKARNULIS, D. M. THOMAS, AND K. IBE, *J. Chem. Soc. Chem. Commun.*, 1603 (1984).
5. G. SHELDRICK, SHELX 76 (program for crystal structure determination), Cambridge (1976).
6. I. D. BROWN AND D. ALTERMATT, *Acta Crystallogr. B* 41, 244–247 (1985).
7. W. WATANABE, Y. FUJIKI, Y. KANAZAWA, AND K. TSUKIMURA, *J. Solid State Chem.* 66, 56–63 (1987).
8. R. CHEARY, submitted for publication.

9. J. E. POST, R. B. VON DREELE, AND P. R. BU-
SECK, *Acta Crystallogr. B* **38**, 1056–1065 (1982).

10. H. U. BEYELER, *Phys. Rev. Let.* **37**, 1557–1560
(1976).

11. W. ABRIEL, F. RAU, AND K.-J. RANGE, *Mater.
Res. Bull.* **14**, 1463 (1979).

12. L. A. BURSILL AND G. GRZINIC, *Acta Crystallogr.
B* **36**, 2902 (1980).

13. PHILIPS EM 420 with field emission gun and super-
twin lense.

14. S. E. KESSON AND T. J. WHITE, *Proc. R. Soc.
London A* **405**, 73 (1986).

15. S. E. KESSON AND T. J. WHITE, *Proc. R. Soc.
London A* **408**, 295 (1986).

16. R. X. FISCHER, *J. Appl. Crystallogr.* **18**, 258
(1985).